Available online at www.sciencedirect.com

ScienceDirect

IFAC Papers Online CONFERENCE PAPER ARCHIVE

IFAC-PapersOnLine 48-11 (2015) 598–603

Robust control of continuous crystallization processes

Rostyslav Geyyer *,** **Achim Kienle** *,** **Stefan Palis** *

* *Otto-von-Guericke University Magdeburg, 39106 Magdeburg, Germany*
** *Max Planck Institute for Dynamics of Complex Technical Systems, 39106 Magdeburg, Germany*

Abstract: In this paper we consider two configurations of continuous crystallization processes with significant nonlinear behaviour and a tendency to self-sustained nonlinear oscillations. The control task is to stabilize the crystallization process in the presence of model uncertainties and external disturbances. This is a challenging task as the model consists of a population balance equation describing the disperse phase, i.e. a nonlinear partial differential equation, being coupled to a mass balance equation describing the liquid phase. In this contribution robust control methods are applied to solve this problem.

Keywords: Control of nonlinear systems, population balance models, robust control.

1. INTRODUCTION

Crystallization is a thermal separation process mostly used in chemical industry that consists in transformation of amorphous solid, liquid or gaseous substance into crystals [Mersmann et al. (2011)]. Crystallization leads to an increase of the concentration and purity of the final product. In this paper continuous crystallization processes within mixed-solution, mixed-product-removal (MSMPR) crystallizers are considered. The focus here is on two important crystallizer configurations: with the fines dissolution loop and without. In order to improve performance of the crystallization process feedback control should be applied. Different control approaches have already been studied: closed-loop control of crystal shape [Ma and Wang (2012)], robust nonlinear control based on the method of moments [Chiu and Christofides (1999)], infinite-dimensional H_∞-control [Vollmer and Raisch (2002)], [Motz et al. (2003)] and discrepancy-based control [Palis and Kienle (2012)]. In this contribution a finite-dimensional robust control approach will be studied resulting in easy implementable low order controllers.

2. CRYSTALLIZATION PROCESS MODELING

In the crystallization processes studied in this contribution crystals are generated and growing due to the oversaturation of the liquid phase: the oversaturated solution is fed to the reactor and cooled down there; such temperature change decreases solvent saturation capacity and causes crystal growth and formation of nuclei. Due to the presence of different effects like seeding, nucleation, fracture, abrasion and growth, crystals have different sizes giving rise to a crystal size distribution (CSD). In many cases the CSD determines the quality of product since many physical properties of the product are closely related to its CSD. In addition, the effectiveness of downstream processing by filtering or drying are strongly influenced by the CSD. Hence, the dynamics of the crystallization process should be studied considering the dynamics of the CSD.

2.1 Continuous crystallization process model derivation

To derive a model of the process the population balance approach [Randolph and Larson (1988)] is applied. Following [Temmel et al. (2014)] a mathematical model was derived with assumptions:

- the reactor content is ideally mixed;
- the solution volume inside the reactor is constant;
- the growth is size-independent;
- the system is diluted the reactor volume is not a function of the substance and crystals mass;
- the mass of the solvent is much higher than the mass of the substance;
- the occurance of breakage or agglomeration can be neglected;
- nuclei have length z_{min} and negligible mass.

The crystal growth and dissolution factor G is assumed to be derived in the following way:

$$G = \begin{cases} K_g \exp(-E_{A,g}/(R_{gas}T))(S-1)^g, & \text{if } S > 1, \\ K_d(S-1), & \text{otherwise,} \end{cases} \tag{1}$$

where the supersaturation S is defined as follows:

$$S(t) = \frac{\omega_l(t)}{\omega_{sat}}. \tag{2}$$

Here, the mass fraction at saturation ω_{sat} was identified experimentally and approximated by a polynomial:

$$\omega_{sat} = \sum_{i=0}^{4} K_i (T - 273.15)^i \tag{3}$$

Peer review under responsibility of International Federation of Automatic Control.
10.1016/j.ifacol.2015.09.252

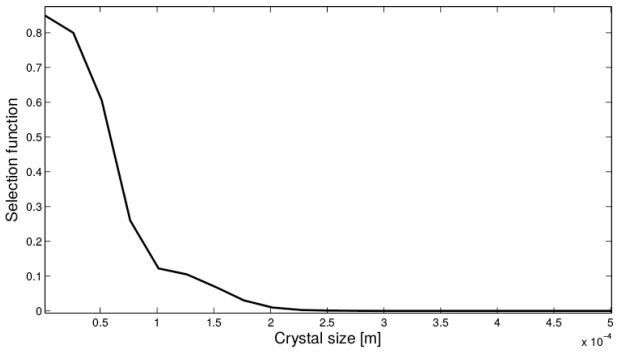

Fig. 1. The fine crystal selection function $R(z)$

The crystal withdrawal term is defined as follows:

$$\dot{n}_{out}(t,z) = \frac{n(t,z)}{\tau_r}, \tag{4}$$

where τ_r represents the residence time.

In one of its configurations the crystallization facility incorporates the fines dissolution loop and the corresponding term is defined:

$$\dot{n}_{diss} = \delta R(z) n_{out}(t,z) \tag{5}$$

The term δ represents the fines dissolution loop rate, the ratio of the product withdrawal related to fines dissolution loop withdrawal and $R(z)$ describes the selection of fine crystals, this function was identified empirically [Temmel (2014)] and is shown in Fig. 1:

$$R(z) = \begin{cases} \dfrac{y_{max}}{(1+\exp(\frac{z-z_f}{w_f})} & \text{if } z < z_{fb}, \\ \dfrac{y_{max}(1+\exp(\frac{z_{fb}-z_b}{w_b}))}{(1+\exp(\frac{z_{fb}-z_f}{w_f}))(1+\exp(\frac{z-z_b}{w_b}))}, & \text{otherwise} \end{cases} \tag{6}$$

The nucleation rate $\dot{n}_{build}$ can be defined as a boundary condition which appears when the supersaturation is greater than one, so the crystals of size z_{min} and negligible mass are generated:

$$Gn|_{z=z_{min}} = \dot{n}_{build}(t) \tag{7}$$

$$\dot{n}_{build}(t,z) = \begin{cases} K_b \exp(-E_{A,b}/(R_{gas}T))(S-1)^b, & \text{if } S > 1, \\ 0, & \text{otherwise} \end{cases} \tag{8}$$

The population balance model for the solid phase of the continuous crystallization is thus defined:

$$\frac{\partial n(t,z)}{\partial t} = -\frac{\partial Gn(t,z)}{\partial z} - \dot{n}_{out}(t,z) - \dot{n}_{diss}(t,z) \tag{9}$$

The mass balance of the solute in the liquid phase is formulated as follows:

$$\begin{aligned} \frac{dm_l}{dt} &= \dot{m}_{l,in}(t) - \dot{m}_{l,out}(t) + \dot{m}_{l,diss,in}(t) \\ &\quad -\dot{m}_{l,diss,out}(t) - k_v \rho_s \frac{d\mu_3(t)}{dt} \end{aligned} \tag{10}$$

where the terms $\dot{m}_{l,in}(t)$ and $\dot{m}_{l,out}(t)$ describe the inward and outward reactor flow, $\dot{m}_{l,diss,in}(t)$ and $\dot{m}_{l,diss,out}(t)$ describe inward and outward fines dissolution loop flow and the last term reflects the crystal growth.

The accumulation term on the left-hand side of the mass balance equation can be substituted in the following way:

$$\frac{dm_l}{dt} = \frac{d(V_r \rho_w \omega_l(t))}{dt} = V_r \rho_w \frac{d\omega_l(t)}{dt}. \tag{11}$$

The inward and outward reactor flows are described as follows:

$$\dot{m}_{l,in}(t) = \dot{V}_{in} \rho_{w,in} \omega_{l,in} = \frac{1}{\tau_r} V_r \rho_{w,in} \omega_{l,in} \tag{12}$$

$$\dot{m}_{l,out}(t) = \dot{V}_{out} \rho_w \omega_l(t) = \frac{1}{\tau_r} V_r \rho_w \omega_l(t) \tag{13}$$

The inward and outward dissolution loop flows are defined as follows:

$$\begin{aligned} \dot{m}_{l,diss,out}(t) &= \dot{V}_f \rho_w \omega_l(t) = \delta \dot{V}_{out} \rho_w \omega_l(t) \\ &= \frac{1}{\tau_r} \delta V_r \rho_w \omega_l(t) \end{aligned} \tag{14}$$

$$\begin{aligned} \dot{m}_{l,diss,in}(t) &= \dot{m}_{l,diss,out}(t) + \frac{k_v \rho_s \dot{V}_f}{V_r} \mu_{3,f}(t) \\ &= \delta \frac{1}{\tau_r} V_r \rho_w (\omega_l(t) + k_v \rho_s \mu_{3,f}(t)) \end{aligned} \tag{15}$$

After some further simplifications the mass balance can be described as follows:

$$\begin{aligned} \frac{d\omega_l(t)}{dt} &= \frac{1}{\tau_r} \left(\frac{\rho_{w,in}}{\rho_w} \omega_{l,in} - \omega_l(t) + \delta k_v \rho_s \mu_{3,f}(t) \right) \\ &\quad - \frac{k_v \rho_s}{V_r \rho_w} \frac{d\mu_3(t)}{dt} \end{aligned} \tag{16}$$

For the process configuration without fines dissolution, the term δ is equal to zero.

2.2 Open-loop simulation

For simulation studies and the following control design the process was discretized applying the finite volume method [Versteeg and Malalasekera (2007)]. The resulting model dimension for controller design was 2000 and for control system validation was reduced to 400 due to the computational expense. In order to gain a rough understanding of the process, simulation studies of the open-loop system were performed. The open-loop simulation expands the knowledge about process peculiarities, its stability, influence of parameter deviations on dynamic behaviour of the model and allows to define qualitative and quantitative indicators of the desired process operation. As we consider two cases, with and without fines

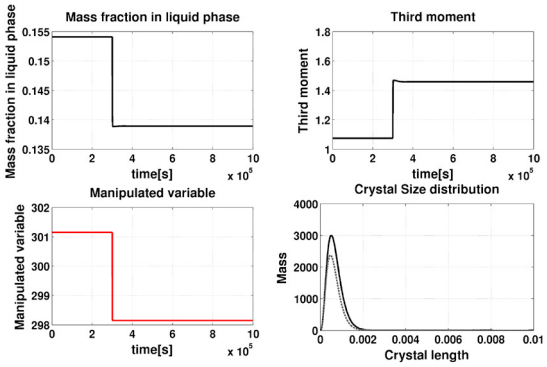

Fig. 2. The configuration without fines dissolution loop - reactor temperature step change $T_r = 301.15K$ to $298.15K$ at $t_{step} = 3 \cdot 10^5 s$

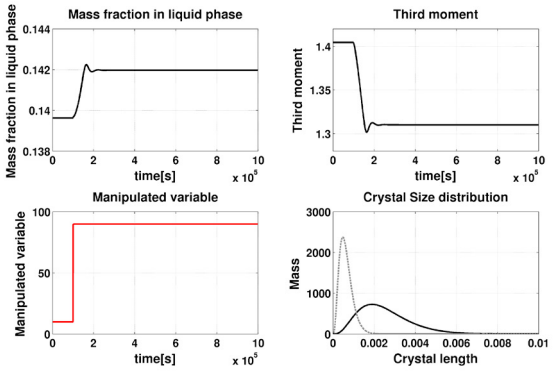

Fig. 3. The configuration without fines dissolution loop - reactor temperature step change $\delta = 10$ to 90 at $t_{step} = 1 \cdot 10^5 s$

dissolution loop, these cases will be analyzed separately. In the configuration without fines dissolution loop, the studied parameter is the temperature within the reactor $T(t)$ which can be controlled by the cooling system. In the second configuration, the fines dissolution loop rate $\delta(t)$ was altered to study different operation points. The model parameters are provided in Table 1. The simulation results are shown in Fig. 2 and 3. In both cases the mass fraction in liquid phase $\omega_l(t)$, the third moment of CSD $\mu_3(t)$, manipulated variable (reactor temperature $T(t)$ for the first configuration and fines dissolution loop rate $\delta(t)$ for the second one) and the CSD $n(t, z)$ - initial distribution (dotted gray) and final distribution (solid black) are shown.

As can be seen the configuration without fines dissolution loop is stable, the configuration with fines dissolution loop shows some oscillatory behaviour but stays stable. However, as has been shown in [Randolph and Larson (1988)] for related configurations the emergence of nonlinear oscillations is possible and should be avoided.

Table 1. Simulation parameters

Parameter	Value
V_r	$0.024m^3$
Q_{out}	$0.1\frac{l}{min}$
K_g	1.67E-006 m/s
g	1.04
$E_{A,g}$	5.71E-009 J/mol
K_b	1234131.27 $1/s$
b	1.1
$E_{A,b}$	5.17E-011 J/mol
K_d	-4.32E-006 m/s
ρ_s	1757 kg/m^3
k_V	0.33
K_0	0.049378679989695
K_1	0.002179443878122
K_2	0.000089305667414
K_3	-0.000002627008140
K_4	0.000000049096298
ρ_w	1000 kg/m^3
z_{min}	1E-6 m

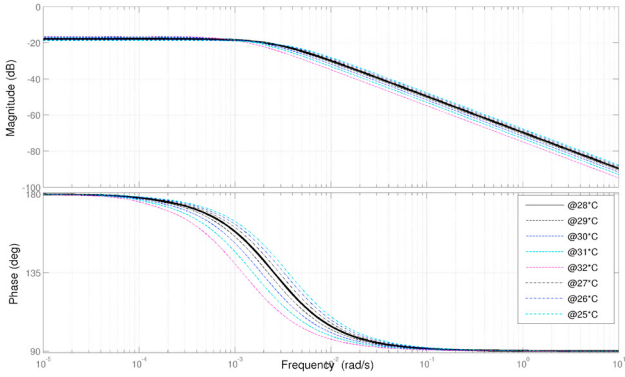

Fig. 4. Bode diagrams for varying reactor temperature (without fines dissolution loop)

3. LINEAR ANALYSIS AND MODEL REDUCTION

3.1 Analysis of the linearized models

The linearization was performed considering both configurations: system without fines dissolution loop and system with it. For a control design appropriate control inputs and outputs should be chosen. Here, for both configurations the third moment μ_3 of the CSD was chosen as the controlled variable. As an appropriate control input the reactor temperature and the fines dissolution loop rate were chosen in the first and second configuration, respectively. Linearization at different operation points for varying reactor temperatures in the range of $298.15K$ to $305.15K$ with nominal model referred to 301.15 and varying fines dissolution loop rate in the range from 10 to 150 with nominal model referred to 90 was undertaken and the results are depicted in figures 4 and 5, respectively with nominal models indicated with wider lines. Both nominal models are stable, controllable and observable. For a direct control design the order is however very high and should be reduced in order to design a low order controller being easily implementable on a programmable logic controller.

3.2 Model order reduction

In this contribution the balanced residualization method has been used for model order reduction [Skogestad and Postlethwaite (2005), Gu (2005), Chiang and Safonov

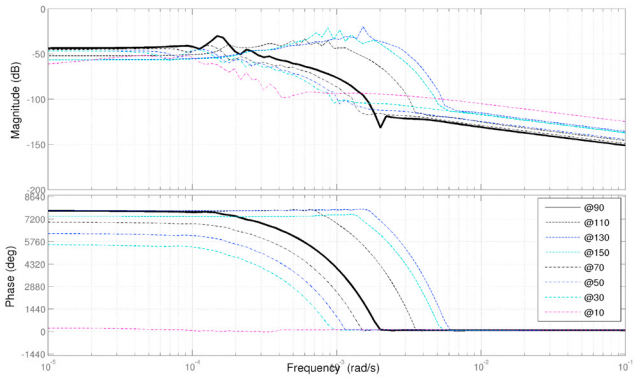

Fig. 5. Bode diagrams for varying dissolution rate (with fines dissolution loop)

(1996)]. For the first configuration a model order reduction to order three and in the second configuration to order 12 was achievable. The approximation error for both reduced order models is relatively small for low frequencies and increases for higher frequencies introducing an additional model uncertainty in the high-frequency zone. This additional model uncertainty should be mitigated by the robustness of the designed controller.

4. ROBUST CONTROLLER DESIGN AND SIMULATION

4.1 H_∞-loop-shaping controller design

Due to the number of considered assumptions, performed simplifications and approximations, a controller should be designed being capable of mitigating mismatches between the real process and the design model. Here, the H_∞-loopshaping approach [McFarlane and Glover (2013)] has been chosen as it combines simplicity, realizability and robustness with respect to the general class of coprime factor uncertainties. As stated earlier for both configurations the third moment μ_3 of the CSD is chosen as the controlled variable and the reactor temperature and the fines dissolution loop rate are the control inputs for the crystallization without and with fines dissolution loop, respectively (Fig. 6).

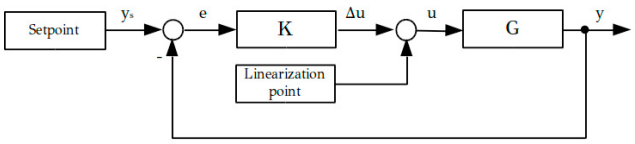

Fig. 6. Control system configuration

In the following it is assumed that the nominal system G is given in its normalized left coprime factorization

$$G = M^{-1}N \tag{17}$$

where M and N are stable coprime transfer functions fulfilling the Bezout identity. Then an uncertain plant G_p consisting of the nominal system G can be represented as follows:

$$G_p = (M + \Delta_M)^{-1}(N + \Delta_N) \tag{18}$$

where Δ_M and Δ_N are stable unknown transfer functions with $\|[\,\Delta_N \;\; \Delta_M\,]\|_\infty < \epsilon$ representing the model uncertainties. It is well known that a controller K robustly stabilizes the perturbed feedback system if it stabilizes the nominal system $G(s)$ and

$$\left\| \begin{bmatrix} K \\ I \end{bmatrix} (I + GK)^{-1} M^{-1} \right\|_\infty \leq \frac{1}{\epsilon}. \tag{19}$$

A coprime factor uncertainty representation is in general superior over additive or multiplicative model uncertainties, as it is not restricted to perturbations which preserve the number of right half-plane poles of the plant. This fact is important for the control of continuous crystallization as stability behaviour may change depending on the specific operating conditions. In order to incorporate requirements on the closed loop performance the above stated H_∞-problem is generally combined with a prior loop shaping stage, where the pre- and postcompensators W_1 and W_2 are designed in order to achieve a desired open loop behaviour. Hence, the H_∞-problem is solved for the nominal model G augmented by the compensators W_1 and W_2

$$G_s = W_2 G W_1 \tag{20}$$

and the H_∞-loop shaping controller K_{res} is formed from the compensators W_1 and W_2 and the solution of the H_∞-problem K.

$$K_{res} = W_1 K W_2 \tag{21}$$

The H_∞-loop-shaping controller design was performed using the reduced-order models taking into account the following requirements: no static error, fast transient and low overshoot. For implementation reasons an additional controller order reduction was performed reducing the order up to 5 and 7, respectively.

4.2 Closed-loop system simulation

The controllers were verified using closed-loop simulations with the full order nonlinear process models. The simulation consisted in reference tracking test to ensure the steady-state accuracy, starting with initial conditions close to the reference point. The reference points are $\mu_3 = 1.3$ for the first configuration and $\mu_3 = 1.4$ for the second one. Then we simulated the emergence of disturbance - increase of feed solution temperature by $\Delta T_{feed} = 0.5K$ at $t = 5 \cdot 10^3 s$ for the first configuration and $t = 2 \cdot 10^6 s$ for the second one. The simulation results are shown in Fig. 7 and 8. The depicted variables are the mass fraction in liquid phase $\omega_l(t)$, the manipulated value $T(t)$ for the first case and $\delta(t)$ for the second one, the third moment of the CSD $\mu_3(t)$ and the crystal size distribution $n(t, z)$: initial (dotted gray) and final (solid black). The crystal size distribution representation over time is depicted in Fig. 9 and 10. Apparently, the system based on model without fines dissolution loop coped with the disturbance with less effect on the process performance than the system based on the second configuration. This is reasonable, because the nature of manipulated variable of reactor temperature is similar to the disturbance nature in contrast to the

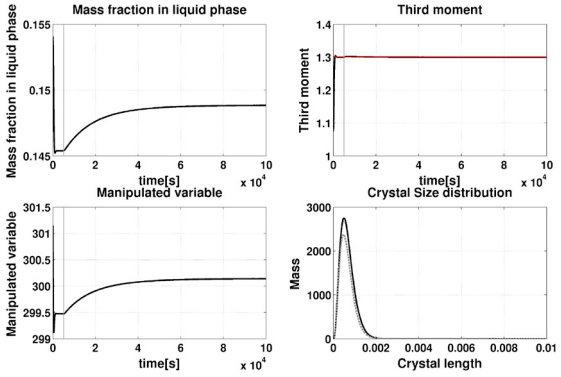

Fig. 7. Controlled crystallization without fines dissolution (disturbance rejection)

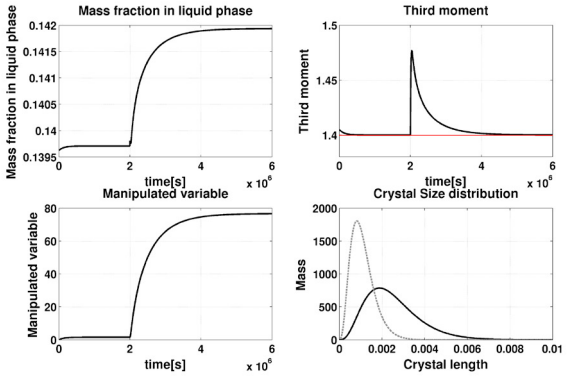

Fig. 8. Controlled crystallization with fines dissolution (disturbance rejection)

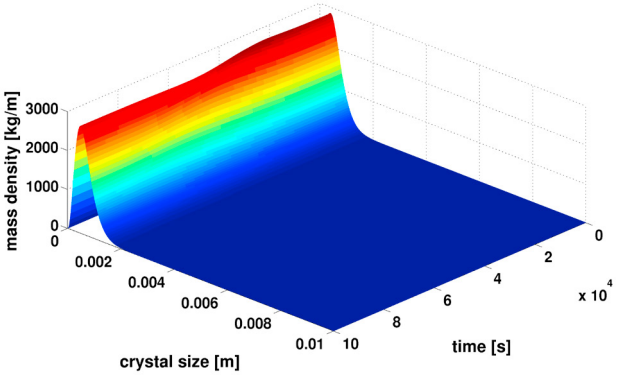

Fig. 9. Controlled crystallization with fines dissolution (disturbance rejection) - crystal size distribution

configuration with fines dissolution loop. Nevertheless, the designed controllers stabilize both process configurations, improve the transient dynamics, mitigate model uncertainties, discretization errors and diminish the influence of unforeseen disturbances as expected.

5. CONCLUSION

In this contribution two configurations of continuous crystallization processes have been studied. Both are described by a nonlinear model with distributed parameters. In order to stabilize the crystallization process and improve its performance feedback control was applied. Here, a linear

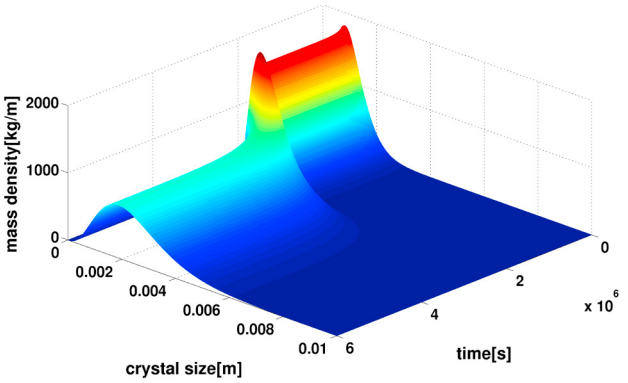

Fig. 10. Controlled crystallization with fines dissolution (disturbance rejection) - crystal size distribution

finite-dimensional robust controller approach being capable of mitigating model uncertainties and diminishing the influence of unforeseen disturbances has been successfully applied. Future work will concern the validation of the designed controllers within the crystallization facility HUGO at the Max Planck Institute for Dynamics of Complex Technical Systems Magdeburg and the extension of the crystallization process model in order to include crystal breakage and agglomeration phenomena.

Table 2. Notation

$n(t,z)$	crystal size distribution
G	crystal growth and dissolution factor
τ_r	residence time
δ	fines dissolution loop rate
$R(z)$	fines dissolution selection function
K_b	fitting parameter for preexponential crystal nucleation rate constant
$E_{A,b}$	activation energy - nucleation
R_{gas}	general gas constant
T	temperature inside reactor
S	supersaturation
b	exponential parameter for nucleation
K_g	fitting parameter for preexponential crystal growth rate constant
$E_{A,g}$	activation energy - growth
g	exponential parameter for growth
K_d	fitting parameter for preexponential crystal dissolution rate constant
$\omega_l(t)$	mass fraction in liquid phase
ω_{sat}	mass fraction at saturation point
k_V	volume shape factor
ρ_s	density of potassium alum
$\mu_3(t)$	the third moment of crystal size distribution
$\mu_{3,f}(t)$	the third moment of fine crystals size distribution
V_r	crystallizer volume
ρ_w	water density
G	nominal plant transfer function
M, N	coprime transfer functions
Δ_M, Δ_N	model uncertainties
ϵ	maximum stability margin
K	H_∞-problem solution
I	identity matrix
W_1, W_2	pre- and postcompensators
G_s	uncertain plant transfer function
K_{res}	resulting H_∞-controller

REFERENCES

Chiang, R.Y. and Safonov, M.G. (1996). *Robust control toolbox : for use with MATLAB : User's guide /.* The

Math Works Inc.
Chiu, T. and Christofides, P.D. (1999). Robust nonlinear control of a continuous crystallizer. *Computers & Chemical Engineering*, 23, Supplement, 257–260.
Gu, D.W. (2005). *Robust Control Design with MATLAB*. Springer Science & Business Media.
Ma, C.Y. and Wang, X.Z. (2012). Closed-loop control of crystal shape in cooling crystallisation of l-glutamic acid. *Journal of Process Control*.
McFarlane, D.C. and Glover, K. (2013). *Robust Controller Design Using Normalized Coprime Factor Plant Descriptions*. Springer, 1 edition.
Mersmann, A., Kind, M., and Stichlmair, J. (2011). *Thermal Separation Technology: Principles, Methods, Process Design*. VDI-Buch. Springer.
Motz, S., Mitrovic, A., Gilles, E.D., Vollmer, U., and Raisch, J. (2003). Modeling, simulation and stabilizing H_∞-control of an oscillating continuous crystallizer with fines dissolution. *Chemical Engineering Science*, 58(15), 3473–3488.
Palis, S. and Kienle, A. (2012). Diskrepanzbasierte regelung der kontinuierlichen kristallisation. *Automatisierungstechnik. - München : Oldenbourg*, 60(3), 145–154.
Randolph, A.D. and Larson, M.A. (1988). *Theory of particulate processes: analysis and techniques of continuous crystallization*. Academic Press.
Skogestad, S. and Postlethwaite, I. (2005). *Multivariable Feedback Control: Analysis and Design*. Wiley-Interscience, 2 edition.
Temmel, E. (2014). Personal communication.
Temmel, E., Lorenz, H., and Seidel-Morgenstern (2014). A short-cut-method for the quantification of crystallization kinetics. *ISIC 2014 - International Symposium on Industrial Crystallization*, 548–550.
Versteeg, H. and Malalasekera, W. (2007). *An Introduction to Computational Fluid Dynamics: The Finite Volume Method*. Prentice Hall, 2 edition.
Vollmer, U. and Raisch, J. (2002). Population balance modelling and $H_\infty-$controller design for a crystallization process. *Chemical Engineering Science*, 57(20), 4401–4414.